Eur. Phys. J. D **32**, 319–328 (2005)
DOI: 10.1140/epjd/e2005-00001-5

THE EUROPEAN PHYSICAL JOURNAL D

The threshold electron impact spectrum of H_2O

J.J. Jureta[a]

Institute of Physics, Pregrevica 118, P.O. Box 68, 11080 Zemun, Serbia and Montenegro

Received 21 July 2004
Published online 18 January 2005 –

Abstract. The threshold electron spectrum of H_2O was obtained using a high resolution electron impact spectrometer combined with the penetrating field method for scattered electrons with energies close to zero eV. The valence, triplet Rydberg states, as well as the resonances were identified and are discussed in the energy region 5.2–14.3 eV. The threshold spectrum confirms the influence of resonances on the enhancement of the intensity of some Rydberg states above 10 eV. The vibrational spacing of the observed transitions of the Rydberg states indicates that the water molecule is excited in the symmetric stretching mode.

PACS. 34.80.Gs Molecular excitation and ionization by electron impact

1 Introduction

Experimental studies of the H_2O molecule by electron impact were very extensive in the period between the sixties and eighties of the last century. The excitation of water molecule by electron impact close to the threshold of the excited states was studied by Schulz [1] using the trapped electron method, Knoop et al. [2] used a double retarding potential difference technique and Compton et al. [3] used the SF_6 trapping (scavenger) method. Their spectra showed some broad features without details, due to poor resolution. Energy-loss studies of H_2O at high impact energy and small scattering angle were performed by Skerbele et al. [4–6], Lasettre et al. [7] and Trajmar et al. [8,9]. Their spectra were in good agreement with the ultraviolet absorption spectra of Price [10], Watanabe and Zelikoff [11] and Gürtler et al. [12]. The most complete energy loss study of H_2O was made by Chutjian et al. [13]. They were able to combine the two modes of operation of energy-loss experiments which includes a large scattering angle and low energy close to the threshold and small scattering angle with high impact electron energy. These two modes of operation allow the possibility of detecting optically forbidden and optically allowed transitions. Despite the systematic work in the past, the assignments of the features in the excitation spectra of H_2O are not yet satisfying.

Threshold electron spectroscopy which uses the penetrating field method was employed for the first time in the present work to study the excitation of water molecules. This method introduced by Cvejanovic and Read [14] and significantly improved in our laboratory has already been applied in studies of the excitation of a number of atomic and molecular species.

Threshold electron spectroscopy is a valuable tool for studying optically forbidden transitions, Rydberg and valence states, as well as negative ions (resonances). This method can be compared only with energy loss experiments at high scattering angle and an electron energy close to the threshold of the excited states.

H_2O is a polar molecule with relatively large dipole moment of 1.85 D. The ground state of H_2O (Herzberg [15]) has the electron configuration $(1a_1)^2(2a_1)^2(1b_2)^2(3a_1)^2(1b_1)^2\ ^1A_1$ where the two last orbitals are occupied orbitals. The first excited electronic states are $(2a_1)^2(1b_2)^2(3a_1)^2(1b_1)(4a_1)\ ^3B_1, ^1B_1$. The promotion of an electron from either the $1b_1$ or $3a_1$ orbital into unoccupied orbitals $3sa_1, 3pa_1$, $3pb_2$ or $3pb_1$ can give sixteen excited Rydberg states. There is also the promotion of an electron from the $1b_1$ or $3a_1$ to the $4a_1$ orbital giving a valence state.

Theoretical calculations relevant to this work were done by Claydon et al. [16] using semi empirical INDO calculations, Winter et al. [17] using extensive configuration interaction studies with other references summarised in this paper, Diercksen et al. [18] using Franck–Condon and static-exchange approximations, Gil et al. [19] using ab initio complex Kohn calculations and Morgan [20] using the R-matrix method.

In the present study the threshold electron spectra of H_2O in the energy region 5.2–14.3 eV was measured. The assignments of the measured features were done according to their energy positions and from comparison with similar data from experimental as well as theoretical results when possible.

[a] e-mail: jureta@fyam.ucl.ac.be

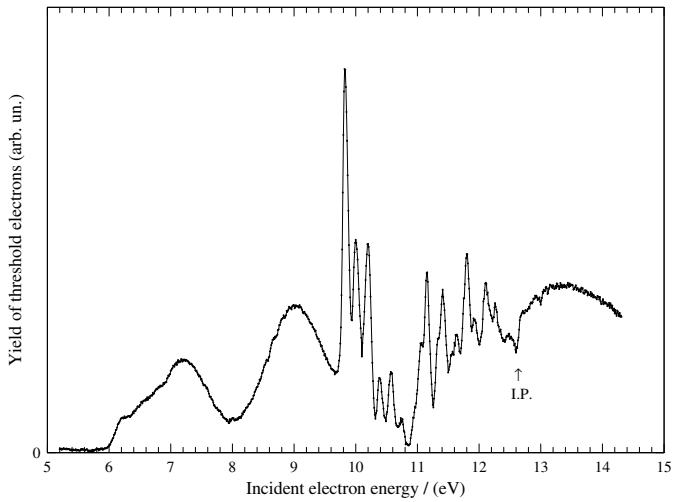

Fig. 1. Threshold electron impact spectrum of H_2O in the energy region 5.2–14.3 eV. The background was subtracted in a linear form.

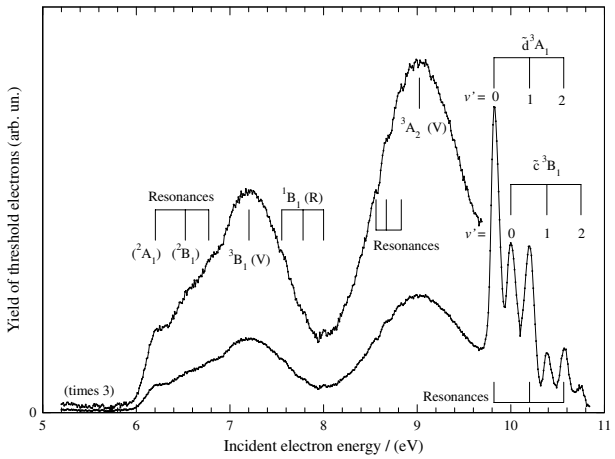

Fig. 2. Part of the threshold spectra from Figure 1 in the energy region 5.2–10.8 eV. The spectrum shows resonances, valence and triplet Rydberg states. The vibrational levels are marked in the form ($v' = 0$, 1 and 2) and it corresponds to (000, 100 and 200) indications noticed in tables and the text.

2 Experimental procedure

The apparatus and experimental procedure were discussed in more details by Cvejanovic et al. [21]. The experimental set-up used to study the excitation process of H_2O ($e + H_2O \rightarrow H_2O^* + e$) is a crossed beam electron spectrometer. It consists of three components, a monochromator with electron gun and lenses, a target region and an analyser with an accompanying lens and detector. The scattered electrons with an energy distribution between zero and 20 meV are trapped by a positive potential from an extractor, analysed by a double cylindrical mirror analyser and detected by a channeltron.

This technique based on the principle of the well-known field penetration method was described in detail by Cvejanovic and Read [14], and further improved by Cvejanovic et al. [22]. The spectrometer operates in four different modes: the constant residual energy mode (CRE), the energy loss mode (EL), the threshold electron spectroscopy mode (TES) and the excitation function mode (EF). In the TES mode, the only mode used in the present study, the detection part was optimised to detect scattered electrons with near zero energy during the sweeping of the incident electron energy. Usually scattered electrons of 10 meV energy were detected which are easy to verify from the measured ratios $2^1S/2^3S$ in the threshold spectrum of helium [14].

The energy scale was calibrated with a mixture of H_2O molecules and xenon with an uncertainty not higher than 10 meV. The current of the incident electron beam was 2 nA. The narrowest peak in the threshold spectrum was 80 meV wide, a poor resolution compared with other threshold spectra obtained with this spectrometer. The reason could be either the absence of a sharp feature in the spectrum, or an uncontrollable influence of the water vapour on parts of the electron optics, including the gas needle in the interaction region.

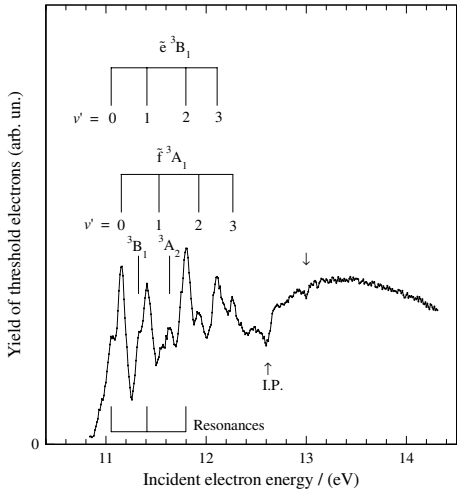

Fig. 3. Part of the threshold spectrum from Figure 1 in the energy region 10.8–14.3 eV. The spectrum shows two Rydberg series, resonances and the ionisation potential in the form of the minimum. The Rydberg series are tentatively assigned on the basis of the vibrational spacing. The weak minimum at 13.0 eV is labelled by an arrow.

3 Results and discussion

The threshold electron spectrum of the water molecule in the energy region 5.2–14.3 eV is shown in Figure 1 with linear subtraction of the background. The figure shows a spectrum composed of two broad maxima and several discrete features below the first ionisation potential. It is a relatively poor spectrum with discrete features compared with the threshold spectra of diatomic molecules. The spectrum is divided into two parts for clarity, the first part in the energy region 5.2–10.8 is shown in Figure 2, while the second part in the energy region 10.8–14.3 eV is shown in Figure 3.

Table 1. Excitation energies (eV) of the H_2O^- negative ion in the energy region 6–12 eV. Comparison with the results of Belic et al. [27], Seng and Linder [23] and Sanche and Schulz [39].

H_2O^-	This work	[27]	[23]	[39]	
Symmetry	E(eV)	E(eV)	E(eV)		E(eV)
$^2A_1$	6.20		6.0		
$^2B_1$	6.52	6.5	6.5		
	6.77				
	8.56	8.6 ($^2A_1$)			
	8.67				
	8.83				
				Band "**a**"	
$v' = 0$	9.82			$v' = 0$	9.92
$v' = 1$	10.20			$v' = 1$	10.33
$v' = 2$	10.56			$v' = 2$	10.69
				Band "**b**"	
$v' = 0$	11.05			$v' = 0$	11.04
$v' = 1$	11.41			$v' = 1$	11.45
$v' = 2$	11.80			$v' = 2$	11.86

3.1 Energy region 5.2–10.8 eV

The main characteristic of this part of the threshold spectrum (Fig. 2) is the existence of two broad maxima situated in the energy regions 6–8 eV and 8–10.8 eV. The first maximum is present without sharp structures, while the second shows six features on the higher energy side. The upper part of Figure 2 shows the part of the spectrum in the energy region between 6 and 9.7 eV in more detail. The assignments of the observed features are listed in Tables 1 and 2.

3.1.1 Energy region 6.0–8.0 eV

This energy region of the water molecule was studied very extensively in the past, both experimentally and theoretically. In the UV spectrum a broad continuum extending from 1860 to 1450 Å (6.665 to 8.550 eV), is present in this energy region. The continuum corresponds to the first member of a ***ns*** Rydberg series [11]. The broad maximum is also found in all other experiments with the electron beam.

In the energy region 6–8 eV, the threshold spectrum in Figure 2 shows a broad non-symmetric maximum, indicating its complex nature. The complexity is the result of detection of near zero energy electrons which originate from two processes, the excitation of electronic states very close to the threshold, and the decay of the negative ions (resonances) releasing slow electrons. Usually these are called non-resonant and resonant contributions in the threshold spectra.

Resonant contribution in the energy region 6.0–8.0 eV

Identification and assignment of the first strong signal which start around 6 eV with the plateau at 6.20 eV is still in dispute. If the result of the theoretical calculation by Claydon et al. [16] is accepted, then the structure should be identified as the first triplet $^3B_1$ state at a calculated energy of 6.2 eV which is in excellent agreement with the energy position of the measured plateau (6.20 eV) in the threshold spectrum. However, other experiments and calculations (see Tab. 2) put the energy of the $^3B_1$ state at around 7.2 eV, which is the argument to believe that the structure at 6.20 eV in the threshold spectrum is not the $^3B_1$ state. Considering that the threshold spectrum detects electrons of low energy released from the decay of a resonance with high efficiency, and a sharp onset of the structure, we believe that the structure at 6.20 eV has a resonant character.

In addition, Seng and Linder [23] suggested the existence of two H_2O^- states in the energy region 6–8 eV, the $^2A_1$ state responsible for vibrational excitation in the 6 eV energy range and the $^2B_1$ state at 6.5 eV responsible for DA processes. These arguments suggest the assignment of the structure at 6.20 to the $^2A_1$ resonance (Tab. 1). This is the first resonance in the H_2O excitation spectra formed in the dipole field of H_2O. The resonance decays to H_2O and an electron which is detected in the threshold spectrum. According to Seng and Linder [23] the resonances are formed as quasi-bound states in the dipole field of H_2O and can be very sharp, assigned as threshold resonances, and very broad, found in an integral excitation functions for symmetric and antisymmetric stretching modes in the energy region from the threshold to 10 eV. Threshold resonances are found in the case of HF and HCl (Rohr and Linder [24]), and they are of general importance in the interaction between electrons and polar molecules.

However, the very broad resonance region in H_2O between 6 and 8 eV can be the result of one or more resonances. These resonances belong to the class of very short lived resonances.

In dissociative attachment (DA) experiments of the H_2O molecule in the energy region above 6 eV, Trajmar

Table 2. Excitation energies (eV) of the observed transitions in the H_2O. Comparison with other experimental and theoretical results.

Excitation	State	This work E(eV)	[13] E(eV)	[2] E(eV)	[17] E(eV)	[18] E(eV)	[43] E(eV)	[9] E(eV)	[44] E(eV)	[34] E(eV)	[1] E(eV)
$b_1 - 4a_1$	$^3B_1$	7.20									
$b_1 - 3sa_1$	$\tilde{a}^3B_1$		7.0	7.2	7.26	7.24	7.22		7.30	6.68	
$b_1 - 3sa_1$	$\tilde{A}^1B_1$	7.55	7.4		7.61					7.30	
		7.78									
		8.00									
$b_1 - 4a_1$	$^3A_2$	9.02									
$b_1 - 3pb_2$	$^3A_2$		8.9	9.1	9.34						9.2
$b_1 - 3pb_1$	$\tilde{d}^3A_1$	9.82 (000)	9.81		9.74			9.81		9.70	
		10.20 (100)									
		10.56 (200)									
$b_1 - 3pa_1$	$\tilde{C}^1B_1$		10.01	10.01	10.06	9.98		10.00	9.90	10.04	10.01
$b_1 - 3pa_1$	$\tilde{c}^3B_1$	10.00 (000)	9.98		9.99					9.96	
		10.38 (100)	10.39								
		10.75 (200)									
$b_1 - 3pa_1$	$\tilde{C}^1B_1$		10.99					10.38			
			10.77					10.76			
$b_1 - 3da_1$	$\tilde{e}^3B_1$	11.05 (000)	11.01							11.05	
		11.41 (100)									
		11.80 (200)									
		12.11 (300)									
$b_1 - 3db_1$	$\tilde{f}^3A_1$	11.15 (000)	11.13							11.16	
		11.53 (100)									
		11.93 (200)									
		12.27 (300)									
$b_1 - 4pa_1$	$^3B_1$	11.32	11.33							11.40	
$b_1 - 4db_2$	$^3A_2$	11.63	11.64							11.64	

et al. [25], Melton [26] and Belic et al. [27] measured the H^- ions. From the last study it can be concluded that H^- ions are released with a kinetic energy between 0.6 and 2.3 eV with a broad maximum between 1.3 and 2.2 eV for an incident electron energy of 6.5 eV. However, we exclude the detection of H^- ions with so high kinetic energy because the analyser for scattered electrons or negative ions in the threshold spectrometer is tuned to detect only those particles with energy close to zero eV.

Valuable theoretical calculations concerning this energy region have been done by [16,17,19,20].

Two other resonant contributions in the threshold spectrum above 6 eV are recognized at energies of 6.52 and 6.77 eV as two weak shoulders of the same form. The signal at 6.52 eV originates from the H_2O^- ion and it can be explained by the detection of near zero electrons released during the decay of this resonance to $H_2O + e$. This resonance is well-known in the literature. It belongs to the Feshbach type with the $^2B_1$ symmetry [25,28] with the $^3B_1$ as the parent state [27] measured at 7.0 eV [13]. The autodetachment width of the resonance is 0.15 eV (Tronc [29]). The threshold spectrum shows the valence $^3B_1$ state at 7.20 eV, suggesting that this state can be the parent state for the resonance at 6.52 eV, but the width of the resonance can not be found because it does not appear as a well defined feature. It should be noted that Claydon et al. [16] calculated a resonance at 6.53 eV and assigned it as $^2A_1$.

The second shoulder at 6.77 eV in the threshold spectrum shows the same form as the former resonance at 6.52 eV, suggesting that it is another resonance in this energy region with the same characteristics as the former resonance. The energy difference between the two shoulders is around 0.25 eV, which is different from vibrational spacing (0.38 eV), found in resonances at higher excitation energies at 10 eV. An additional argument for assigning this shoulder to a resonance comes from the calculations of Morgan [20], who found a sharp resonance at 6.785 eV in $^2B_1$ symmetry, suggesting that it corresponds to the resonance at 6.5 eV by shifting the excitation thresholds to their experimental values. The threshold spectrum shows that this energy correction in her calculations was not necessary because the original position of the structure is in good agreement with measured structure in the threshold spectrum. The threshold spectrum in the present form gives no further information on this resonance. Finally, the existence of three resonances in the threshold spectrum in the 6–7 eV range confirms the idea of Seng and

Linder [23] of the existence of one or more resonances in this energy region.

Non-resonant contribution in the energy region 6.0–8.0 eV — the valence state

The top of the broad maximum in the threshold spectrum at an energy of 7.20 eV is tentatively assigned as the $^3B_1(b_1 - 4a_1)$ valence state due to its form, which is typical for the valence states, and theoretical calculations [19,20]. In the calculation of the cross-sections for this state, Morgan [20] found a narrow resonance at an energy of 8.81 eV as the dominant feature and a weak resonance at 12.7 eV. From the threshold spectrum it can be concluded that the broadening and intensity of the structure can be a consequence of either the mixing of the valence and Rydberg states or from a resonant contribution. Until now the results of theoretical calculations and experiments have given no clear answer in the assignment of the first excited electronic state in the water molecule. The $^3B_1$ state was assigned as the first Rydberg state in most of the optical and energy-loss experiments. However, the theoretical calculations [19,20] treat this state as a valence state. According to these calculations, the excitation of either a $1b_1$ or $3a_1$ electron into the lowest unoccupied $4a_1$ virtual orbital can give the triplet and singlet valence states $^3B_1, ^1B_1, ^3A_1$ and $^1A_1$. For the $^3B_1$ and $^1B_1$ valence states calculated energies of 7.445 and 7.885 eV were found. From the form of the first maximum in the threshold spectrum at 7.2 eV it can be concluded that it has a valence character assigned as $^3B_1$, but there is no evidence of the presence of the singlet $^1B_1$ state.

The energy position of the first Rydberg $\tilde{a}^3B_1(b_1 - 3sa_1)$ state from measurements [2,13] and a theoretical calculation [17] are presented in Table 2. It is clear that a good agreement exist between our measurements and the cited references. However Table 2 shows disagreement in the position of the energy of the $^3B_1$ state between energy loss measurements [13], (7.0 eV) and the threshold spectrum (7.20 eV). This disagreement suggests the existence of both valence and Rydberg states in this energy region, as is the case in the threshold spectrum of oxygen in the energy region 7–9 eV [30]. The above discussion shows the complexity of this energy region of the water molecule and requires a new experimental technique in order to resolve this problem.

At the higher energy side of the first maximum, the threshold spectrum shows two weak shoulders at energies of 7.55, 7.78 eV and a small peak at 8.0 eV. These three features have not been seen in any energy loss experiments. Additionally, they are also not predicted by theoretical calculations. Due to the absence of similar data in the literature for comparison and the above discussion of the existence of Rydberg and valence state in this energy region, we assigned them as arising from the vibrational levels of the Rydberg $\tilde{A}^1B_1(b_1 - 3sa_1)$ state. This state has been well established in optical spectra at 7.49 eV, which is in good agreement with energy loss experiments at high impact energy and small scattering angle [13], but theoretical calculations [17] found a value of 7.61 eV. It should be noted that this transition is an optically allowed transition and hence it can not be strong in the threshold spectrum.

3.1.2 Energy region 8.0–9.8 eV

This energy region of the water molecule has been studied in optical and energy loss experiments. In both techniques, the region is dominated by a broad maximum without sharp structures. The threshold spectrum (Fig. 2) shows a broad symmetric maximum at an energy of 9.02 eV with three weak shoulders at the lower energy side. The broad form of the maximum indicates its complexity. As in the case of the first maximum between 6 and 8 eV, the complexity is a consequence of resonant and non-resonant contributions.

Resonant contribution in the energy region 8.5–8.8 eV

The resonant contribution is recognised in the energy region of the three shoulders (8.56, 8.67 and 8.83 eV) as three resonances with a spacing of 0.11 and 0.16 eV, respectively. Electrons are formed in the process of the decay of the H_2O^- negative ion to $H_2O + e$. The energy position of the resonance at 8.56 eV is in good agreement with the resonance at 8.6 eV found by Belic et al. [27] in measurements of the DA process in H_2O. The resonance has a $^2A_1$ symmetry [31] with the b^3A_1 Rydberg state as the parent. Nothing can be said about the width of this resonance from the threshold spectrum but the parent can be the $^3A_2$ valence state at 9.02 eV. It should be noted that H^- ions at 8.6 eV found in the DA process [27] can not be detected by threshold spectroscopy because they are released with a kinetic energy of 3 eV.

There are no data in literature for the second resonance at 8.67 eV. From the threshold spectrum it can be seen that it has the same form as the former resonance at 8.56 eV, suggesting that it belongs to this resonance as the second vibrational level.

The third resonance at 8.83 eV coincides in energy with the resonance found by Morgan [20]. In her calculations she found a pronounced narrow resonance at 8.81 eV with a width of 0.025 eV of $^2A_1$ symmetry described as a "core excited shape resonance". Upon the correction of the energy scale in her calculation, the energy of the resonance was 8.59 eV which was the argument to suggest that it corresponds to the dissociative attachment process found by Belic et al. [27]. It seems that this correction of the energy scale was not necessary.

Comparing the lifetimes of the different resonances in the threshold spectrum we can conclude that the resonances in the 8.5–8.8 eV range have much longer lifetimes than the resonances in the 6–7 eV range because they are presented in the form of a progression of three vibrational levels. Nothing can be said about the autodetachment width of the resonances in these two energy regions because they are not well defined in the threshold spectrum. It should be noted that Tronc [29] found that the

autodetachment width of the resonance at 8.6 eV is larger than that of the resonance at 6.5 eV.

It is interesting to note that Chutjian et al. [13] found a series of bands in the form of weak shoulders in the energy region 8.6–9 eV at residual energies of 2.0 eV for H_2O and 0.5 eV for D_2O, with a spacing of 0.15 eV, which is similar to the value from our threshold spectrum. The authors suggested that they belong to vibrational levels of the lowest-lying $^3A_2$ state. The conclusion was made on the basis of only two residual energies. However, they did not give the energy positions for this band, so it is not possible to make a comparison between their results and the present study.

Non-resonant contribution in the energy region 8.0–9.8 eV — valence state

The non-resonant contribution to the second broad maximum is manifested at an energy of 9.02 eV, corresponding to the top of this maximum which is tentatively assigned as the $^3A_1(b_1 - 4a_1)$ valence state according to its form and a theoretical calculation [20]. In this calculation the $^3A_1$ valence state was found at 9.286 eV. The results of other theoretical calculations for the cross-section of this state [32,33] are compared with the calculation of Morgan [20]. Very little agreement was found between these theories. The cross-section curve of Morgan [20] shows a well defined threshold and a sharp $^2B_2$ resonance at 12.7 eV.

From the threshold spectrum it can not be concluded which contribution dominates in the region of a broad maximum, resonant or non-resonant. In addition, it can not be concluded whether there is any contribution from the singlet valence $^1A_1$ state, calculated by Morgan [20] at an energy of 9.996 eV, and the $^3A_2$ Rydberg state.

The $^3A_2$ (b_1-3pb_2) Rydberg state was found in energy-loss measurements [13] at 8.9 eV and by theoretical calculations at 9.34 [17] and 8.68 eV [34]. Table 2 shows the disagreements in the energy positions for this state. The disagreements suggest new measurements in order to find accurate energy position of this state.

The threshold spectrum does not show the existence of the singlet $^1A_2(b_1 - 3pb_2)$ Rydberg state predicted by theoretical calculation [17] at 9.46 eV and at 9.1 eV in energy loss measurements [13].

The intensity ratio between the two maxima peaked at 9.02 and 7.20 eV in the threshold spectrum has a value of 1.59 (calculated from the zero of the vertical scale). This is different to the intensity ratio of almost 1 obtained in energy loss experiments at a residual energy of 0.5 eV [13]. At higher residual energies (2.0 eV), this ratio is less than 1. This dramatic change in the intensity of the two maxima as a function of the residual electron energy is a consequence of the influence of a resonant contribution.

3.1.3 Energy region 9.8–10.8 eV

This energy region of the threshold spectrum shown in Figure 2 is characterized by six discrete features superimposed on the higher energy side of the second maximum at 9.02 eV. The features show anomalies in their intensities indicating that they are influenced by a resonant contribution. The features are tentatively assigned according to their energy positions, vibrational spacing and from a comparison to similar data of experimental and theoretical results.

Non-resonant contribution in the energy region 9.8–10.8 eV — Rydberg states

The three features regularly spaced at energies of 9.82, 10.20 and 10.56 eV are tentatively assigned as the $\tilde{d}^3A_1$ $(b_1 - 3pb_1)$ Rydberg state according to their similar form in the threshold spectrum, energy position of the first vibrational level and vibrational spacings of 0.38 and 0.36 eV, respectively. The spacing is very close to the spacing of the symmetric stretching mode of the H_2O^+ (0.397 eV [35,36]). This is the first time that a threshold spectrum shows three vibrational levels of the triplet $^3A_1$ state in this regular form which has not been seen in any energy loss experiment. The possible explanation is that it belongs to an optically forbidden transition strongly excited at the threshold energies. The intensity enhancement is the consequence of the resonant contribution. The resonance has the same excitation energy as this state (see discussion bellow).

The first feature at an energy of 9.82 eV appears in the threshold spectrum as the most intense feature and is assigned as the $^3A_1$ state (000) $(v' = 0)$ transition. Table 2 shows a good agreement in the energy position between this work and energy loss experiments [9,13] (9.81 eV), but not with theoretical calculations [17,34]. This feature is not seen by optical spectroscopy. The very strong enhancement of this feature in the threshold spectrum is the consequence of the resonant contribution. Namely, the first vibrational level of the resonance coincides in energy with the $^3A_1$ state and is responsible for its enhancement. Due to this resonance contribution, it is not possible to conclude which contribution of these two is dominant in its intensity.

It is interesting to note that this feature appears in energy loss experiments at low residual energy only, and its intensity is a function of the residual energy [13]. At a residual energy of about 2 eV, the feature appears with a small intensity and reaches maximum intensity close to the threshold energy. Trajmar et al. [9] concluded that the feature at 9.81 eV belongs to the triplet $\tilde{d}^3A_1$ state on the basis of its angular distributions and intensity ratios. The authors believe that this state could be important in the radiation chemistry of aqueous solutions.

The second feature at an energy of 10.20 eV is assigned as the (100) $(v' = 1)$ transition of the $^3A_1$ state according to the spacing of 0.38 eV. Its intensity is also the consequence of a resonant contribution. The feature was seen neither in the energy-loss measurements nor by optical spectroscopy. The closest feature with an energy of 10.16 eV was seen in [13] and theoretical calculations [17,34] assigned as the $\tilde{D}^1A_1$ (000) state.

The third feature at an energy of 10.56 eV is assigned as the third member (200) $(v' = 2)$ of the $^3A_1$ state. The

enhancement of the feature is the consequence of underlying resonance. In energy-loss measurements [13], the feature at 10.55 eV was assigned as $\tilde{D}^1A_1$ (100) state.

The theoretical calculation of Winter et al. [17] confirms only the existence of the $\tilde{d}^3A_1$ state at an energy of 9.74 eV. It should be noted that the threshold spectrum does not show the existence of the singlet $\tilde{D}^1A_1(b_1 \rightarrow 3pb_1)$ state in a form seen in both energy-loss experiments [4,9,13] and in optical spectroscopy [10,11,37].

The $\tilde{c}^3B_1(b_1 - 3pa_1)$ Rydberg state

The three features at energies of 10.00, 10.38 and 10.75 eV (Fig. 2) are tentatively assigned as the $\tilde{c}^3B_1$ Rydberg state according to their energy positions and the vibrational spacing of 0.38 and 0.37 eV, respectively (Tab. 2). The vibrational spacing of 0.38 eV corresponds well to the vibrational spacing of the symmetric stretching mode of the H_2O^+ (0.397 eV, [35,36]). The first transition (000) ($v' = 0$) at an energy of 10.00 eV is in excellent agreement with the energy position predicted by a theoretical calculation [17] and an energy loss result [13] (Tab. 2). Its energy position and intensity indicate that it belongs to the triplet state, an optically forbidden transition with enhanced intensity in the threshold spectrum. Moreover, the spectrum shows no direct influence of the resonance to the intensity of this feature. Hence, we assigned the first (000) transition as the $\tilde{c}^3B_1$ state. In an energy loss experiment at the low residual energy of 2 eV, Chutjian et al. [13], observed the triplet component of the $\tilde{C} \leftarrow \tilde{X}$ transition at an energy of 9.98 eV. This transition was not seen in other energy-loss experiments.

The transition (100) ($v' = 1$) at 10.38 eV seen in Figure 2, with a lower intensity than the peak at 10.00 eV, is assigned as the second member of the $\tilde{c}^3B_1$ state, bearing in mind that threshold spectroscopy emphasizes optically forbidden transitions. This identification is in accordance with the result of Chutjian et al. [13]. These authors observed a strong feature at 10.39 eV in an energy-loss experiment at a residual energy of 2 eV, suggesting that it belongs to the $\tilde{c}^3B_1$ triplet state.

It should be noted that the energy positions of the (000) and (100) transitions of the triplet $\tilde{c}^3B_1$ state are in good agreement with the energies of the (000) and (100) transitions of the singlet $\tilde{C}^1B_1$ $(b_1 - 3pa_1)$ state (Tab. 2), found in energy-loss experiments [9,13] and by optical spectroscopy [37,38]. From energy-loss spectroscopy [4] and ultraviolet spectroscopy [10,11], the states at 10.00 and 10.39 eV were assigned as the $A_1 v' = 0$ and 1, respectively.

The third member (200) ($v' = 2$) of the $\tilde{c}^3B_1$ state at 10.75 eV is seen in Figure 2 as a feature of low intensity. The assignment of this feature was determined taking into account its energy position and energy spacing of 0.36 eV.

The (200) transition of the singlet $\tilde{C}^1B_1$ state was found in energy loss experiments [9,13] at energies of 10.76 and 10.77 eV, respectively and by optical spectroscopy [37] at an energy of 10.765 eV. In an energy-loss experiment [4], the feature at 10.76 eV was assigned as the A_1 $v' = 2$ state.

It should be noted that the threshold spectrum does not show the existence of the singlet component of the B_1 state ($\tilde{C}^1B_1$), which is not the consequence of the lack in resolution of the spectrometer (0.08 eV). The calculated singlet-triplet splitting is of 0.07 eV [17].

The threshold spectrum does not show the feature at 10.68 eV found in an energy-loss experiment [13] at a residual energy of 2 eV. The feature was assigned as the $^3A_2 \leftarrow \tilde{X}$ transition.

Resonant contribution in the energy region 9.8–10.7 eV

The threshold spectrum (Fig. 2) clearly shows the enhancement of the three features at energies 9.82, 10.20 and 10.56 eV. Their enhancements are the consequence of the existence of core excited resonance of H_2O^- present in the form of the three vibrational levels with energies which coincide with the energies of the Rydberg states (Tab. 1). The vibrational spacings of 0.38 and 0.36 eV correspond well with the vibrational spacing of the $\tilde{c}^3B_1$ state, indicating that this state is the parent state of this resonance. The spacing of 0.38 eV is very close to the vibrational spacing of H_2O^+ in the symmetric stretching mode (0.397 eV).

It is interesting to note that Sanche and Schulz [39] could not measure the resonance seen in the threshold spectrum, but they predicted the existence of this resonance on the basis of the existence of a small peak at an energy of 9.78 eV. They proposed that the $^1B_1$ state can form a resonance progression. The threshold spectrum confirms this idea except that the $\tilde{c}^3B_1$ state is the parent state. They measured another resonant progression called band "**a**" with three vibrational levels at 9.92, 10.33 and 10.69 eV (Tab. 1) with the $^1A_1$ state at 10.17 eV as the parent state.

3.2 Energy region 10.8–14.3 eV

This energy region of H_2O has not been studied as systematically either in energy-loss experiments or in theoretical calculations as the first part of the spectra below 10 eV. Only, the energy-loss experiment of Chutjian et al. [13] gives assignments of the features found in this energy region based on the results of some energy-loss experiments as well as theoretical calculations of Winter et al. [17] and Goddard et al. [34]. In the energy-loss experiments at a residual energy of 2 eV, Chutjian et al. [13] could not obtain the sharp features, but their spectrum could be compared with our threshold spectrum because they detect electrons with small residual energy. As a result and in the absence of similar threshold spectra with high resolution, the assignments of the measured features in the threshold spectrum were limited to the above cited references.

This energy region of the threshold spectrum presented in Figure 3 clearly shows two distinct Rydberg series converging to the first ionization potential at 12.610 eV. Both series show vibrational levels equally spaced, but some of them show intensity anomalies influenced by the presence of underlying resonance. The assignment of the series is done mostly according to the vibrational spacing between

the measured features and by comparison with similar data in the literature, when possible [13]. It should be noted that the assignment of the features in this energy region is very chaotic throughout the literature because of the absence of systematic studies, both experimental and theoretical.

Resonant contribution in the energy region 11.05–11.8 eV

This energy region of the threshold spectrum as does the one between 9.8–10.7 eV, shows the existence of core excited resonance in the form of the three vibrational levels at energies of 11.05, 11.41 and 11.80 eV (Tab. 1). These energies coincide with energies of the $\tilde{e}^3B_1$ Rydberg series which causes their enhancements. The vibrational spacing of 0.36 and 0.39 eV is very close to the vibrational spacing of the next $\tilde{e}^3B_1$ Rydberg series, indicating that this state is the parent state of this resonance.

The existence of the resonance in this energy region of water molecule was found by Sanche and Schulz [39] (Tab. 1). The resonant band called band "**b**" has three vibrational levels at energies close to the energies in the threshold spectrum. From the vibrational spacing of 0.41 eV, they concluded that it comes from the symmetric stretching vibration of the H_2O^- ion. However, they could not make an unambiguous assignment of the band "**b**" but they proposed that the state F [15] at 11.12 eV is the parent state of this band . This prediction is confirmed in the threshold spectrum, where the $\tilde{e}^3B_1$ Rydberg state at 11.15 eV is recognised as the parent state of this resonance. According to these authors, the formation of the core excited resonances in a water molecule takes place through the promotion of the essentially non-bonding $1b_1$ electron to a non-bonding Rydberg orbital. The incident electron is temporary bound in another Rydberg orbital. This can explain why the zero levels of both bands "**a**" and "**b**" have a large probability of formation.

It should be noted that in the energy region of this resonance at 11.8 eV, the third peak of the H^- ion was also observed in a dissociative attachment experiment [27]. This resonance was assigned as $^2B_2$ without more details. Again, as in the previous case, the H^- ion can not be detected with the present technique due to its high kinetic energy.

Non-resonant contribution in the energy region 11.0–12.3 eV — Rydberg states

The features of the threshold spectrum (Fig. 3) at energies 11.05, 11.41, 11.80 and 12.11 eV are tentatively assigned as vibrational levels (000, 100, 200 and 300, respectively) of the $\tilde{e}^3B_1(b_1 - 3da_1)$ Rydberg state. The assignment was done according to the energy position and the vibrational spacing of 0.36, 0.39 and 0.31 eV, respectively (Tab. 2). The vibrational spacing is close to the vibrational spacing of a symmetric stretching mode of the H_2O^+ (0.397 eV).

The first feature at 11.05 eV is present in the threshold spectrum in the form of a shoulder not separated from the next feature at 11.15 eV due either to a resonant contribution, which changes the form of the feature, or to the poor resolution of the spectrometer. The threshold spectrum does not give a definite conclusion for this behaviour. Table 2 shows an excellent agreement in the energy position of this feature with that calculated by Goddard et al. [34]. This feature was not seen in the energy-loss spectra at high impact energies. Only at the low residual energy of 2 eV, did Chutjian et al. [13] notice a broad weak transition in the region of 11.0 eV, which they proposed belongs to the $\tilde{e}^3B_1$ $(b_1 - 3da_1)$ state.

The second two features (100 and 200) at energies 11.41 and 11.80 eV, respectively, are present in the threshold spectrum with enhanced intensity due to the strong influence of resonance. Hence, their assignments as members of the $\tilde{e}^3B_1$ Rydberg state is based only on the vibrational spacing of 0.39 eV, which corresponds to the vibrational spacing of the symmetric stretching mode of the H_2O^+.

In a energy-loss experiment at low residual energy, Chutjian et al. [13] found features at energies of 11.40 and 11.78 eV and assigned them as the $^1A_1$ $(b_1 - 4pb_1)$ and $^1A_1(b_1 - 4db_1)$ states, respectively, according to a theoretical calculation of Goddard et al. [34] (11.48 eV). In the ultra violet absorption spectra [10], the features at 11.413 and 11.790 eV were assigned as the B_2 and D_2 states, respectively.

The last member of the $\tilde{e}^3B_1$ Rydberg state (300) at an energy of 12.11 eV appears in the spectrum with a smaller intensity than the previous features because its intensity is not under the influence of resonance. The vibrational spacing between the (200 and 300) transitions is 0.31 eV, which is little bit lower than the vibrational spacing between the first two transitions (0.39 eV). This can be explained by deformation of the spectra in the region close to the ionization potential where the other series converge.

The $\tilde{f}^3A_1(b_1 - 3db_1)$ Rydberg state

The next four features in the threshold spectrum (Fig. 3) at energies 11.15, 11.53, 11.93 and 12.27 eV with vibrational spacings of 0.38, 0.40 and 0.34 eV respectively are tentatively assigned as the (000, 100, 200 and 300) members of the $\tilde{f}^3A_1$ $(b_1 - 3db_1)$ Rydberg state (Tab. 2). As in the first series, the assignment for this series is done according to energy position and vibrational spacing, which is very close to the vibrational spacing of the symmetric stretching mode of the H_2O^+ (0.397 eV). All other features are present with low intensity except for the first one.

The first feature (000) at 11.15 eV has an enhanced intensity in the threshold spectrum due to the influence of an underlying resonance. The energy position of this feature is very close to the energy position of the feature at 11.16 eV calculated by Goddard et al. [34] and assigned as the $\tilde{f}^3A_1(b_1 - 3db_1)$ state. A feature with this assignment was found by Chutjian et al. [13] at an energy of 11.13 eV. Optical spectroscopy does not show the existence of a feature at this energy.

The (100) vibrational level at 11.53 eV is of a weak intensity probably due to a perturbation by resonance at 11.41 eV or poor resolution of the spectrometer. Exactly at this energy Chutjian et al. [13] found a feature assigned as the $^1B_1$ ($b_1 - 5sa_1$) state according to a calculation of Goddard et al. [34] (11.66 eV). In optical spectroscopy [11,40], the feature at 11.52 eV was assigned as the $^1B_1$ state.

The next two features (200 and 300) at energies of 11.93 and 12.27 eV, respectively, have similar forms and intensities in the threshold spectrum with a vibrational spacing of 0.34 eV, which was the argument to assign them as members of the $\tilde{f}^3A_1$ state. Chutjian et al. [13] found a feature at an energy of 11.92 eV and assigned it as the $^1B_1$ ($3a_1 - 3pb_1$) state according to a theoretical calculation of Winter et al. [17]. This feature was not seen by optical spectroscopy. The feature at 12.27 eV was seen neither in energy-loss measurements nor by optical spectroscopy.

The two weak features in the threshold spectrum (Fig. 3) at energies of 11.32 and 11.63 eV do not belong to the neighbouring Rydberg series and they were identified and assigned according to their energy positions, which correspond to energies of measured features in an energy-loss experiment [13] (Tab. 2). In this way, the feature at 11.32 eV in the form of a shoulder is assigned as the $^3B_1$ ($b_1 - 4pa_1$) Rydberg state according to Chutjian et al. [13] (11.33 eV) and Goddard et al. [34] (11.40 eV). The feature at 11.63 eV is assigned as the $^3A_2$ ($b_1 - 4db_2$) Rydberg state, also according to [13] (11.64 eV) and [34] (11.64 eV).

3.2.1 Energy region 12.0–14.3 eV

The first ionization potential of the water molecule (12.610 eV [15]) is clearly indicated in the threshold spectrum in the form of a minimum at an energy of 12.605 eV. The minimum is not as deep as in case of rare gas atoms due to the convergence of the Rydberg series to higher ionization potentials but is much better defined than in the case of molecular oxygen [30]. Above the ionization potential, the threshold spectrum shows no discrete features arising from the excitation except a weak minimum at 13 eV. Contrary to this, optical spectrum [12] shows a large number of discrete features above the first ionization potential, indicating that the threshold technique is not sensitive to optically allowed transitions.

The weak minimum which appears at 13.00 eV coincides in energy with the second step in the absorption cross-section spectra of water vapour [40] at 13.023 eV. The energy difference between this step and the ionization potential is 3200 cm^{-1} (0.397 eV), which corresponds well to the frequency of 3170 cm^{-1} (0.393 eV) of the few excited states above the first ionization potential in the absorption cross-section spectrum. No further explanation for this step can be found in literature. The weak minimum in the threshold spectrum indicates the energy position of the opening of a new channel for another excited state in the ground state of the H_2O^+. The energy spacing between the minimum and the first ionization potential is 0.395 eV, which is very close to the vibrational spacing of the Rydberg series of H_2O which converges to the first ionization potential and to the frequency of the symmetric stretch mode of the H_2O^+ (0.397 eV) [35, 36]. This strongly supports the prediction of Price [10] and Mulliken [41] of the same stability for both H_2O and H_2O^+. It is due to the electron configuration of the ground state of H_2O where the most loosely bound orbital is the nonbonding $1b_1$ orbital. Hence, the promotion of one electron from this orbital can not change configuration of the final state and both H_2O and H_2O^+ should have the same stability.

The second ionization potential of H_2O at 14.35 eV [42] is not shown in the figure.

4 Conclusion

Using a threshold electron spectrometer combined with the detection of scattered electrons with very low energy, the electron impact spectrum of the water molecule in the energy region 5.2–14.3 eV was studied. The whole threshold spectrum is characterized by several energy regions. In the energy region 6–10 eV, the spectrum shows two broad maxima without discrete features assigned as the $^3B_1$ and $^3A_2$ valence states and resonances formed in the strong dipole field. The mixture of resonant and non-resonant contributions including both valence and Rydberg states makes this region very complicated to understand. Hence, a new more sensitive method is necessary in order to separate these different contributions.

The first discrete Rydberg series were identified and assigned as the $^3A_1$ ($b_1 - 3pb_1$) and $\tilde{c}^3B_1$ ($b_1 - 3pa_1$) states in the energy region 10–11 eV. A resonant contribution was recognized by the intensity enhancement of the $^3A_1$ state. Two Rydberg series converging to the first ionization potential at 12.610 eV were tentatively assigned as the $\tilde{e}^3B_1(b_1 - 3da_1)$ and $\tilde{f}^3A_1(b_1 - 3db_1)$ in the energy region 11–14.3 eV. The weak minimum at 13.0 eV, with an energy spacing of 0.395 eV above the first ionization potential confirms the excitation of H_2O in the symmetric stretching mode. Good agreement was found in the energy positions of the measured triplet states with the measurement of Chutjian et al. [13] in an energy-loss experiment at low residual energy.

We wish to acknowledge to Dr. V. Bocvarski and Dr. V. Cvjetkovic for their participation in the data treatment and Dr. B. Marinkovic for his critical reading of the paper. This work was partly supported by project 1424 of MNZZS–Serbia and COST Action P9-RADAM. We acknowledge Dr. S. Cvejanović for his role in designing the threshold spectrometer and obtaining the raw data.

References

1. G.J. Schulz, J. Chem. Phys. **33**, 1661 (1960)
2. F.W.E. Knoop, H.H. Brongersma, L.J. Osterhoff, Chem. Phys. Lett. **13**, 20 (1972)

3. R.N. Compton, R.H. Huebner, P.W. Reinhardt, L.G. Christophorou, J. Chem. Phys. **48**, 901 (1968)
4. A. Skerbele, V.D. Meyer, E.N. Lassettre, J. Chem. Phys. **43**, 817 (1965)
5. A. Skerbele, E.N. Lassettre, J. Chem. Phys. **44**, 4066 (1966)
6. A. Skerbele, M.A. Dillon, E.N. Lassettre, J. Chem. Phys. **49**, 5042 (1968)
7. E.N. Lassettre, A. Skerbele, M.A. Dillon, K.J. Ross, J. Chem. Phys. **48**, 5066 (1968)
8. S. Trajmar, W. Wiliams, A. Kuppermann, J. Chem. Phys. **54**, 2274 (1971)
9. S. Trajmar, W. Wiliams, A. Kuppermann, J. Chem. Phys. **58**, 2521 (1973)
10. W.C. Price, J. Chem. Phys. **4**, 147 (1936)
11. K. Watanabe, M. Zelikoff, J. Opt. Soc. Am. **43**, 753 (1953)
12. P. Gürtler, V. Saile, E.E. Koch, Chem. Phys. Lett. **51**, 386 (1977)
13. A. Chutjian, R.I. Hall, S. Trajmar, J. Chem. Phys. **63**, 892 (1975)
14. S. Cvejanovic, F.H. Read, J. Phys. B: At. Mol. Phys. **7**, 1180 (1974)
15. G. Herzberg, *Electronic Spectra and Electronic Structure of Polyatomic Molecules* (Van Nostrand, Princeton, NJ, 1967)
16. C.R. Claydon, G.A. Segal, H.S. Taylor, J. Chem. Phys. **54**, 3799 (1971)
17. N.W. Winter, W.A. Goddard III, F.W. Bobrowicz, J. Chem. Phys. **62**, 4325 (1975)
18. G.H.F. Diercksen, W.P. Kraemer, T.N. Rescigno, C.F. Bender, B.V. McKoy, S.R. Langhoff, P.W. Langhoff, J. Chem. Phys. **76**, 1043 (1982)
19. T.J. Gil, T.N. Rescigno, C.W. McCurdy, B.H. Lengsfield III, Phys. Rev. A **49**, 2642 (1994)
20. L.A. Morgan, J. Phys. B: At. Mol. Opt. Phys. **31**, 5003 (1998)
21. S. Cvejanović, J. Jureta, M. Minic, D. Cvejanović, J. Phys. B: At. Mol. Phys. **25**, 4337 (1992)
22. S. Cvejanović, J. Jureta, D. Cvejanović, J. Phys. B: At. Mol. Phys. **18**, 2541 (1985)
23. G. Seng, F. Linder, J. Phys. B: At. Mol. Phys. **9**, 2539 (1976)
24. K. Rohr, F. Linder, J. Phys. B: At. Mol. Phys. **9**, 2521 (1976)
25. S. Trajmar, R.I. Hall, J. Phys. B: At. Mol. Phys. **7**, L458 (1974)
26. Ch. Melton, J. Chem. Phys. **57**, 4218 (1972)
27. D. Belic, M. Landau, R.I. Hall, J. Phys. B: At. Mol. Phys. **14**, 175 (1981)
28. R. Azria, Y. Le Coat, G. Lefevre, D. Simon, J. Phys. B: At. Mol. Phys. **12**, 679 (1979)
29. M. Tronc, thesis, Université Paris-XI, Orsay, France (1973)
30. J.J. Jureta, S. Cvejanović, Eur. Phys. J. D **30**, 37 (2004)
31. A.M. Weiss, M. Krauss, J. Chem. Phys. **52**, 4363 (1970)
32. H.P. Pritchard, V. McKoy, M.A. Lima, Phys. Rev. A **41**, 546 (1990)
33. M.T. Lee, S.E. Michelin, L.E. Machado, L.M. Brescansin, J. Phys. B: At. Mol. Opt. Phys. **28**, 1859 (1995)
34. W.A. Goddard III, W.J. Hunt, Chem. Phys. Lett. **24**, 464 (1974)
35. C.R. Brundle, D.W. Turner, Proc. Roy. Soc. Lond. A **307**, 27 (1968)
36. A.W. Pots, W.C. Price, Proc. Roy. Soc. Lond. A **326**, 181 (1972)
37. S. Bell, J. Mol. Spectr. **16**, 205 (1965)
38. J.W.C. Jones, Can. J. Phys. **41**, 209 (1963)
39. L. Sanche, G.J. Schulz, J. Chem. Phys. **58**, 479 (1973)
40. K. Watanabe, A.S. Jursa, J. Chem. Phys. **41**, 1650 (1964)
41. R.S. Mulliken, J. Chem. Phys. **3**, 506 (1935)
42. W.C. Price, T.M. Sugden, Trans. Far. Soc. **44**, 108 (1948)
43. D. Yeager, V. McKoy, G.A. Segal, J. Chem. Phys. **61**, 755 (1974)
44. R.J. Buenker, S.D. Peyerimhoff, Chem. Phys. Lett. **29**, 253 (1974)